Angewandte Chemie
Eine Zeitschrift der Gesellschaft Deutscher Chemiker

Supporting Information

69451 Weinheim, Germany

Mesostructured Prussian Blue Analogues

Xavier Roy,[a] Laurence K. Thompson,[b] Neil Coombs,[c] and Mark J. MacLachlan,[a]*

[a] *Department of Chemistry, University of British Columbia, 2036 Main Mall,*
Vancouver, BC V6T 1Z1.

[b] *Department of Chemistry, Memorial University of Newfoundland, St. John's, NL*
A1B 3X7.

[c] *Centre for Nanostructure Imaging, Department of Chemistry, University of Toronto,*
80 St. George St, Toronto, ON M5S 3H6.

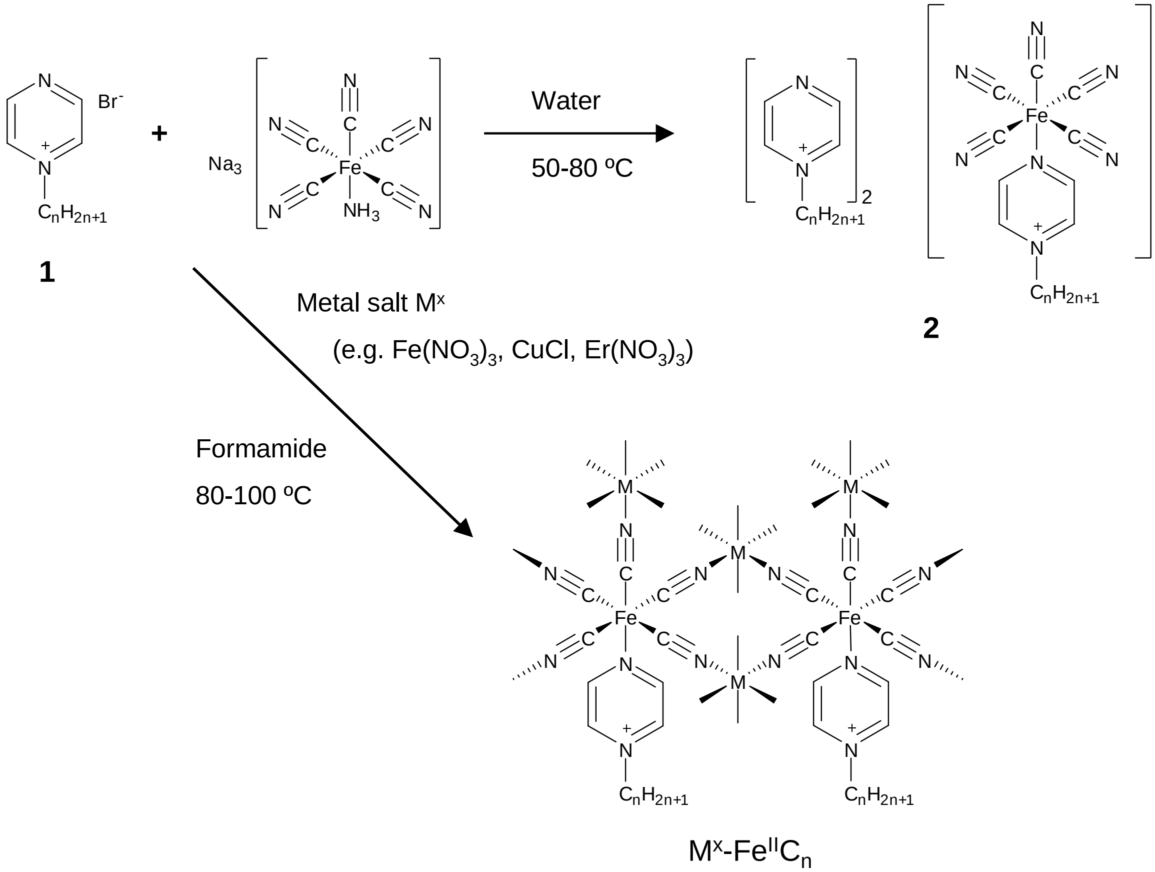

Scheme S1. Synthetic routes to complex **2** and M^x-$Fe^{II}C_n$.

1 Synthesis and characterization of the starting materials

The new alkylpyrazinium bromides (**1**) were synthesized using a modified literature preparation[1] previously used to prepare analogues with shorter chains. A four-fold excess of pyrazine was added to the bromoalkane in N,N-dimethylformamide. The mixture was stirred at 60°C for 2-3 days and the product was precipitated with diethyl ether, filtered and recrystallized from cold ethanol. Typical yield: 30%.

1.1 Dodecylpyrazinium bromide

^{1}H NMR (400 MHz, [D$_4$]MeOH, 25°C): δ= 9.50 p.p.m. (d, 2H; CH), 9.14 (d, 2H; CH), 4.73 (t, ^3J(H,H) = 7.8 Hz, 2H; CH$_2$), 2.09 (m, 2H; CH$_2$), 1.43 (m, 2H; CH$_2$), 1.30 (m, 16H; CH$_2$), 0.91 (t, ^3J(H,H) = 7.0 Hz, 3H; CH$_3$); Elemental Analysis: Calc'd (%) for $C_{16}H_{29}N_2Br$: C 58.35, H 8.88, N 8.51; found: C 58.70, H 9.15, N 8.56.

1.2 Tetradecylpyrazinium bromide

^{1}H NMR (400 MHz, [D$_4$]MeOH, 25°C): δ 9.50 p.p.m. (d, 2H; CH), 9.14 (d, 2H; CH), 4.72 (t, ^3J(H,H) = 7.8 Hz, 2H; CH$_2$), 2.08 (m, 2H), 1.43 (m, 2H; CH$_2$), 1.30 (m, 20H; CH$_2$), 0.91 (t, ^3J(H,H) = 6.8 Hz, 3H; CH$_3$); Elemental Analysis: Calc'd (%) for $C_{18}H_{33}N_2Br$: C 60.50, H 9.31, N 7.84; found: C 60.86, H 9.63, N 8.00.

1.3 Hexadecylpyrazinium bromide

^{1}H NMR (400 MHz, [D$_4$]MeOH, 25°C): δ 9.50 p.p.m. (d, 2H; CH), 9.14 (d, 2H; CH), 4.73 (t, ^3J(H,H) = 7.8 Hz, 2H; CH$_2$), 2.09 (m, 2H; CH$_2$), 1.43 (m, 2H; CH$_2$), 1.30 (m, 24H; CH$_2$), 0.91 (t, ^3J(H,H) = 6.8 Hz, 3H; CH$_3$); Elemental Analysis: Calc'd (%) for $C_{20}H_{37}N_2Br$: C 62.32, H 9.68, N 7.27; found: C 62.46, H 9.76, N 7.5.

1.4 Octadecylpyrazinium bromide

^{1}H NMR (400 MHz, [D$_4$]MeOH, 25°C): δ 9.50 p.p.m. (d, 2H; CH), 9.13 (d, 2H; CH), 4.72 (t, ^3J(H,H) = 7.8 Hz, 2H; CH$_2$), 2.08 (m, 2H; CH$_2$), 1.43 (m, 2H; CH$_2$), 1.30 (m, 28H;

CH_2), 0.91 (t, ${}^3J$(H,H) = 6.8 Hz, 3H; CH_3); Elemental Analysis: Calc'd (%) for $C_{22}H_{41}N_2Br$: C 63.91, H 9.99, N 6.78; found: C 64.18, H 10.30, N 6.64.

1.5 Icosylpyrazinium bromide

^{1}H NMR (400 MHz, [D_4]MeOH, 25°C): δ 9.50 p.p.m. (d, 2H; CH), 9.12 (d, 2H; CH), 4.71 (t, ${}^3J$(H,H) = 7.8 Hz, 2H; CH_2), 2.08 (m, 2H; CH_2), 1.43 (m, 2H; CH_2), 1.29 (m, 32H; CH_2), 0.91 (t, ${}^3J$(H,H) = 7.0 Hz, 3H; CH_3); Elemental Analysis: Calc'd (%) for $C_{24}H_{45}N_2Br$: C 65.29, H 10.27, N 6.34; found: C 65.46, H 10.40, N 6.62.

1.6 Docosylpyrazinium bromide

^{1}H NMR (400 MHz, [D_4]MeOH, 25°C): δ 9.50 p.p.m. (d, 2H; CH), 9.12 (d, 2H; CH), 4.71 (t, ${}^3J$(H,H) = 7.8 Hz, 2H; CH_2), 2.08 (m, 2H; CH_2), 1.43 (m, 2H; CH_2), 1.29 (m, 36H; CH_2), 0.91 (t, ${}^3J$(H,H) = 7.0 Hz, 3H; CH_3); Elemental Analysis: Calc'd (%) for $C_{26}H_{49}N_2Br$: C 66.50, H 10.52, N 5.97; found: C 66.72, H 10.90, N 6.06.

1.7 Sodium amminepentacyanoferrate(II)

$Na_3Fe(CN)_5NH_3 \cdot 3H_2O$ was prepared from sodium nitroprusside according to the procedure by Kenney et al.[2] The yellow solid was recrystallized from a solution of ammonium hydroxide and methanol.

2 Synthesis and characterization of complex 2

2.1 Synthesis of complex **2**

To a large excess of the alkylpyrazinium bromide dissolved in hot water (50-80 °C, depending on the alkyl chain length) was added dropwise an aqueous solution of $Na_3Fe(CN)_5NH_3 \cdot 3H_2O$. A blue precipitate usually formed immediately. If it did not, the solution was cooled down until the solid started to appear. The slurry was stirred at that same temperature for 1 h and then hot filtered and washed with hot water. A blue solid was obtained. The solid was redissolved in EtOH, filtered to remove insoluble material, and dried under vacuum. The product is a blue solid.

2.2 Characterization of complex **2** (n = 18)

^{1}H NMR (400 MHz, [D$_4$]MeOH, 25°C): δ= 9.91 p.p.m. (d, 2H; CH), 9.57 (d, 4H; CH), 9.26 (d, 4H; CH), 7.97 (d, 2H; CH), 4.88 (4H; overlapping with the residual H_2O peak), 4.00 (t, ^3J(H,H) = 7.4 Hz, 2H; CH_2), 2.14 (m, 4H; CH_2), 1.99 (m, 2H; CH_2), 1.32 (m, 90H; CH_2), 0.93 (t, ^3J(H,H) = 6.8 Hz, 9H; CH_3).

Figure S1 shows the typical NMR spectrum for unlinked complex **2** (n = 18). Apart from the peaks below 1.8 ppm corresponding to the alkyl chain, two sets of peaks integrating in a ratio of 2:1 are observed for each pyrazinium proton. These data indicate that complex **2** has two alkylpyrazinium cations (**C**) and one alkylpyrazinium coordinated to the pentacyanoferrate(II) (anion **A**) as shown in Scheme S1. Electrospray ionization mass spectrometry (ESI-MS) was used to confirm this result. Figure S2 shows the typical

ESI-MS spectrum in negative mode for unlinked complex **2** (n = 18) which is composed of two singly charged cations (**C**) and one doubly charged anion (**A**). The peak at *m/z* 520.4 corresponds to the protonated anion [**A**•H$^+$]$^-$, while the species [**C**•**A**]$^-$ is observed at *m/z* 853.2. The two sets of peaks at *m/z* 686.6 and 742.0 correspond to the aggregates [**C**•**A**$_2$•H$^+$]$^{2-}$ and [**C**$_2$•**A**$_3$•H$^+$]$^{3-}$, respectively. No peaks due to partial hydrolysis are observed.

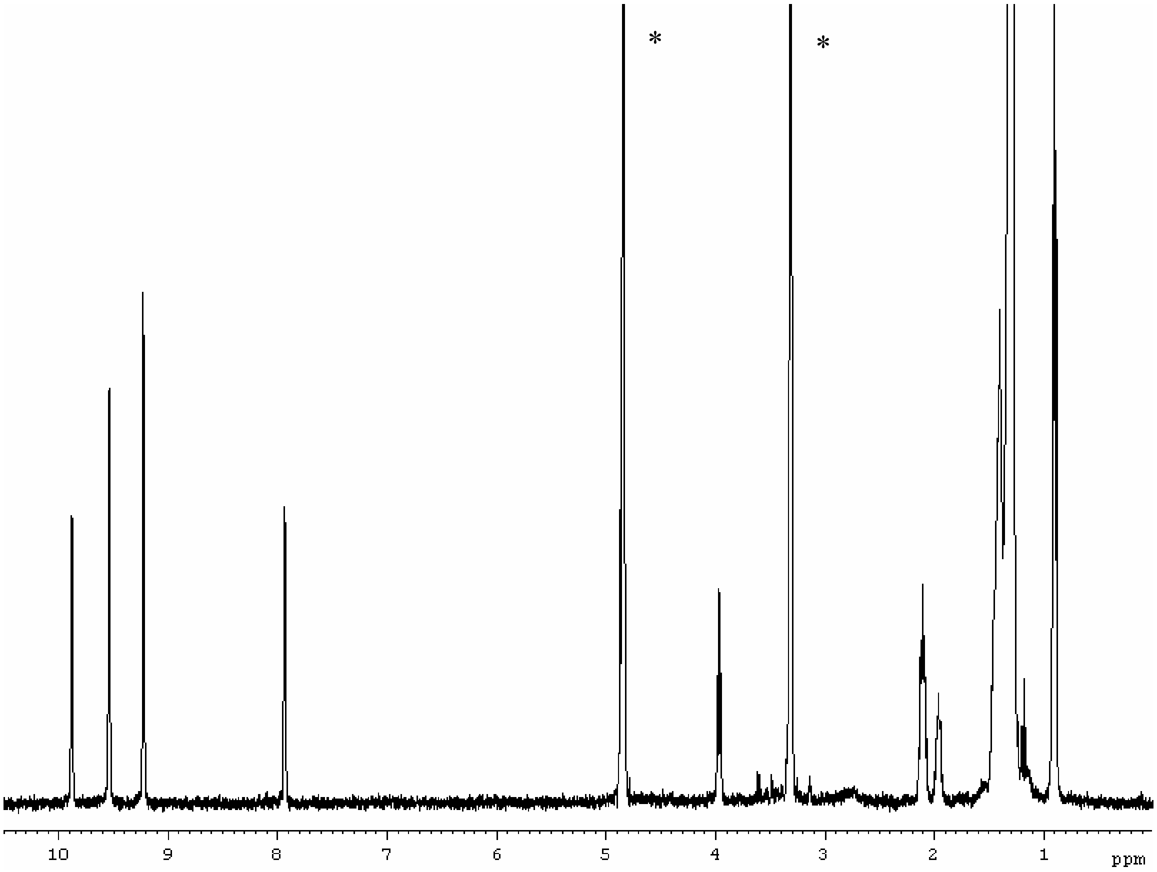

Figure S1. ^{1}H NMR (400 MHz, [D$_4$]MeOH, 25°C) spectrum for unlinked complex **2** (n = 18). * denotes peaks from NMR solvent. The NMR spectrum shows a trace of ethanol impurity (3.6 and 1.2 ppm).

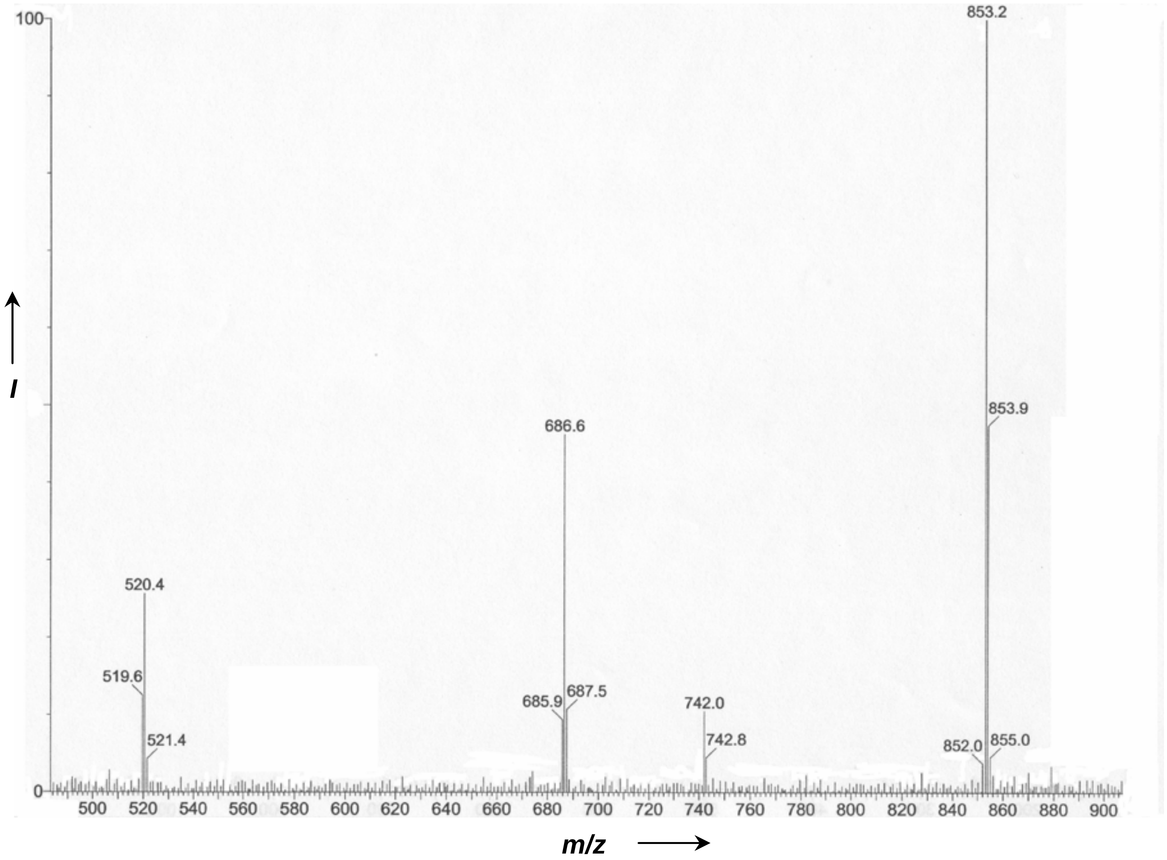

Figure S2. ESI-MS (negative mode) of unlinked complex **2** (n = 18).

3 Synthesis of M^{x}-$Fe^{II}C_n$

The general synthetic procedure to prepare the mesostructured PB analogues is presented here. A more detailed representative example can be found in the Methods section of the article.

One equivalent of $Na_3Fe(CN)_5NH_3{\cdot}3H_2O$ in formamide was added dropwise to a large excess of the alkylpyrazinium bromide (5 to 15 equiv.) dissolved in hot formamide (80 °C for C_{12}-C_{18} chains; 100 °C for C_{20} and C_{22}). The solution instantaneously turned dark blue and was stirred for ten minutes. A large excess of the metal salt in hot formamide was then added dropwise to the stirred solution. The solution was stirred for 10 mins and then allowed to stand at room temperature for 12 h. The product was isolated on a fine fritted funnel, washed with formamide (80 °C), boiling ethanol, and water (80 °C), then dried under vacuum. In the case of some metal salts, additional formamide was necessary to dissolve the metal salt. We prepared materials using $Fe(NO_3)_3$, $Cu(NO_3)_2$, CuCl, $Ni(NO_3)_2$, $Mn(O_2CCH_3)_2$, $Zn(NO_3)_2$, $Gd(NO_3)_3$, $Er(NO_3)_3$, and other metal complexes – in every case a mesostructured product was obtained. When an unreactive (inert) metal salt (e.g., chromium(III)) was used, then no precipitate formed. Table S1 provides analytical data and PXRD information for a variety of the samples.

4 Equipment

The 300 MHz and 400 MHz ^{1}H NMR spectra were recorded on Bruker AV-300 and AV-400dir spectrometers, respectively. The powder X-ray diffraction (PXRD) patterns were obtained using a Bruker D8 Discover equipped with a CuKα sealed tube X-ray source. A Hitachi-2000 scanning transmission electronic microscope (STEM) operating at 200 kV was used to image the materials. Some pictures were obtained in high angle annular dark field (HAADF) mode. Infrared (IR) spectra were obtained using a Thermo Scientific Nicolet 4700 FTIR spectrophotometer. The samples were dispersed in a potassium bromide matrix and transmission was measured in the range 400-4000 cm^{-1}. The UV-vis spectra were recorded on a Varian Cary 5000 spectrophotometer. The samples were dispersed in a potassium bromide matrix and absorbance was measured in the range 200-2000 nm. The spectra were fitted using the software PeakFit to calculate the peak positions and the full width at half maximum. Mössbauer spectroscopy was performed on a WEB Mössbauer spectroscopy system equipped with a Janis Research variable temperature SH1-850 cryostat, closed cycle refrigerator and a ^{57}Co in Rh matrix source (~ 40 mCi). The powder was loaded into a custom-made Teflon holder. The Mössbauer spectrum of the sample was taken at 300 K. The velocity was scanned between 8 and -8 mm s^{-1} using a constant acceleration triangular waveform. Magnetic measurements were collected over the range of 2-300 K using a Quantum Design MPMS5S Squid magnetometer operating at 0.1 T and corrected for diamagnetic contributions of the sample holder. The C, H and N elemental analyses were obtained at the UBC Microanalytical Services Laboratory and the metal analyses were performed by Canadian

Microanalytical Service Ltd. using ICP-MS of digested (boiling H_2SO_4/HNO_3) samples. The ESI-MS spectra were also obtained at the UBC Microanalytical Services Laboratory using a Waters ZQ mass spectrometer coupled with a Waters Alliance 2695 delivery system. Energy-dispersive X-ray (EDX) spectroscopy was performed using a Hitachi S-3000N scanning electron microscope (SEM) equipped with a Quartz Xone EDX system.

5 IR spectroscopy

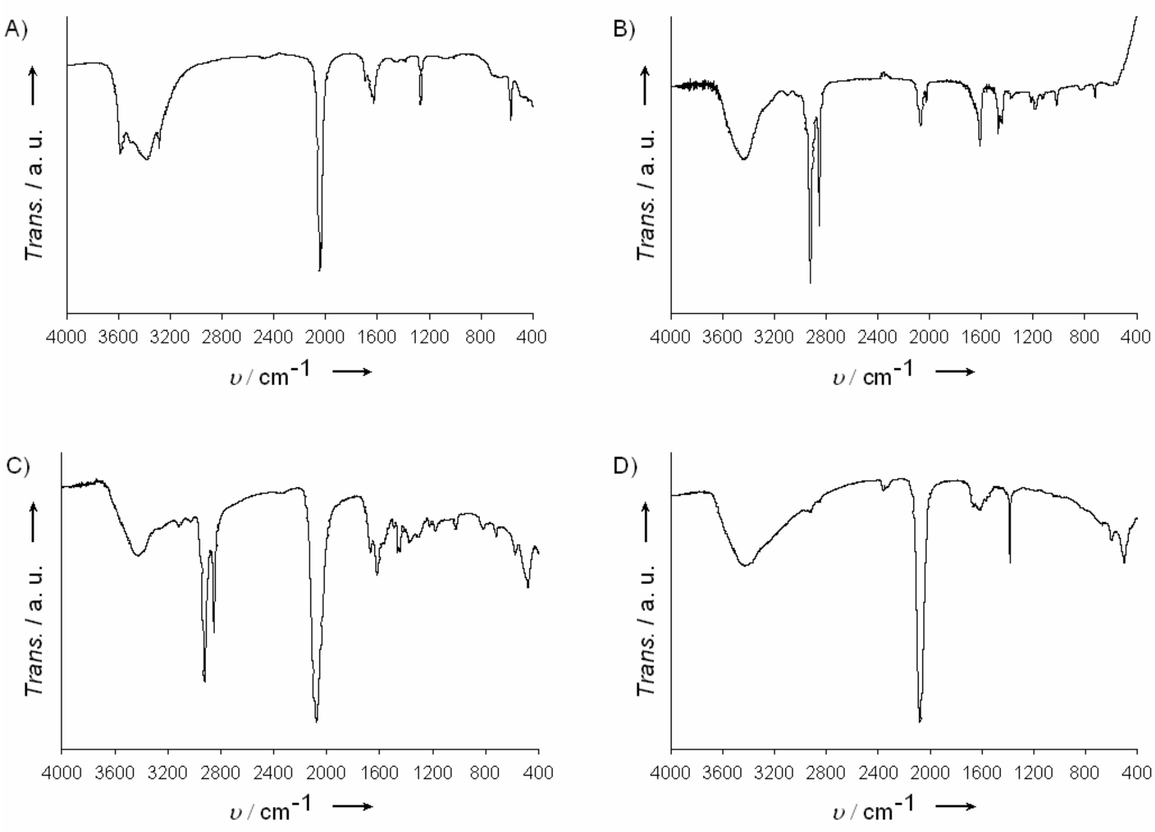

Figure S3. FTIR spectra. **A** shows Na$_3$Fe(CN)$_5$NH$_3$·3H$_2$O, **B** Unlinked complex **2** (n = 18), **C** Fe^{III}-Fe^{II}C$_{18}$ and **D** bulk PB. The ν_{CN} stretching modes are observed in the range 1950-2150 cm^{-1}.

6 Elemental composition and structural properties

Table S1. Elemental composition and structural properties of a series of mesostructured PB analogues.

Sample	% C	% H	% N	% Fe	% M	1^{st} PXRD peak (Å)	Mesostructure (from PXRD)
Fe^{III}-$Fe^{II}C_{12}$	38.83	4.98	18.40	24.00		~35	**
Fe^{III}-$Fe^{II}C_{14}$	42.29	5.70	16.96	21.50		~37	**
Fe^{III}-$Fe^{II}C_{16}$	44.12	6.48	15.23	18.00		~38	**
Fe^{III}-$Fe^{II}C_{18}$	49.63	7.57	13.01	15.70		39.0	Hexagonal
Fe^{III}-$Fe^{II}C_{20}$	40.63	6.10	10.18	17.77		40.1	Hexagonal
Fe^{III}-$Fe^{II}C_{22}$	59.22	9.14	9.99	9.97		44.7	Hexagonal
Er^{III}-$Fe^{II}C_{12}$	40.53	5.74	15.43	9.68	20.92*	37.4	Hexagonal
Er^{III}-$Fe^{II}C_{18}$	48.50	7.14	13.48	7.79	19.18*	42.7	Lamellar
Er^{III}-$Fe^{II}C_{22}$	50.77	7.57	11.61	6.01	12.63*	46.2	Lamellar
Cu^{I}-$Fe^{II}C_{18}$	48.19	6.57	10.29	4.66	15.57*	38.6	Cubic
Cu^{II}-$Fe^{II}C_{18}$	47.28	6.51	10.78	4.72	14.10	40.2	Cubic
Gd^{III}-$Fe^{II}C_{18}$	48.54	7.41	13.86			42.1	Lamellar
Mn^{II}-$Fe^{II}C_{18}$	46.69	7.09	10.77	5.82	10.80	43.1	Hexagonal
Ni^{II}-$Fe^{II}C_{18}$	55.64	8.03	13.25	4.77	7.17	37.1	Lamellar
Zn^{II}-$Fe^{II}C_{18}$	50.53	7.26	11.48			34.4	**

* obtained by EDX analysis by measuring the atomic ratio relative to Fe. ** Phase could not be accurately determined as only 1 peak was observed in the PXRD pattern.

7 Complete reference 1b) for Main Text

[1] b) J. S. Beck, J. C. Vartulli, W. J. Roth, M. E. Leonowicz, C. T. Kresge, K. D. Schmitt, C. T. W. Chu, D. H. Olson, E. W. Sheppard, S. B. McCullen, J. B. Higgins, J. L. Schlenker, *J. Am. Chem. Soc.* **1992**, *114*, 10834-10843.

8 Supporting Information References

[1] C. T. Bahner, L. L. Norton, *J. Am. Chem. Soc.* **1950**, *72*, 2881-2882.

[2] D. J. Kenney, T. P. Flynn, J. B. Gallini, *J. Inorg. Nucl. Chem.* **1961**, *20*, 75-81.